

## ANALYSING THE LOCUS OF PATIENTS MOVEMENT FOR REGISTRATION OF THERMAL IMAGES IN BREAST EXAMINATION

Stephenson de Sousa Lima GALVÃO<sup>1</sup>, Huilan LI<sup>2</sup>, Aura CONCI<sup>3</sup> and Trueman  
MACHENRY<sup>4</sup>

<sup>1</sup>Instituto Federal de Educação, Ciência e Tecnologia do Piauí (IFPI), Brazil

<sup>2</sup>School of Mathematical Sciences, Shandong Normal University, Ji'nan, Shandong, P.R. China,

<sup>3</sup>Computer Institute, Federal Fluminense University, Brazil

<sup>4</sup>Department of Mathematics and Statistics, York University, Canada.

**ABSTRACT:** A thermal camera captures heat pattern radiated by the skin surface that can serve as important indicators for medical diagnostic. Analyzing and interpreting thermo-grams have been increasingly employed in the diagnosis and monitoring of breast diseases thanks to its non-invasive, non-harmful nature and low cost. It is called mammothermography and has been very effective in the early detection of breast cancer especially when dynamic protocol is used in acquiring the patient data. However, during the acquiring time, the patients do some small movements that cause differences between their images. These differences if not correct can results in error in the computational analyses. Therefore, approaches to align the images and undo these differences must be the first step in computational analyze of these thermo-grams. This correction is known as image registration, it uses transformation functions to match different images. To achieve a proper development of a registration tool for help in the real time visualization and diagnosis we need first to know well the problem. The use of very generic or incorrect function to undo this displacements increase the processing time and even do not promote adequate results. In this work, we study the movements performed by patients during dynamic acquisition to find a pattern of possible movements and faults in the images sequence. After this, we show that the rigid body transformation can align the patients' images properly. These functions are tested in a database of patients' images. Results show that together rotations and translations can corrects possible difference among the patients' images.

**Keywords:** dynamic infrared image, image registration; thermo-grams, affine transformation, rigid body transformation

### 1. INTRODUCTION

A thermal camera captures heat pattern radiated by the skin that can serve as important indicators in medical diagnostic. Thanks to the advances in infrared (IR) thermal imaging technology, image processing techniques, and the understanding of thermo-grams, IR is very suitable for use as a supplement to health monitoring and clinical diagnosis. Analyzing

and interpreting thermo-grams has been increasingly employed in the diagnosis and monitoring of breast diseases thanks to its non-invasive, non-harmful nature and low cost [1]. It is called mammothermography and has been very effective in the early detection of breast cancer.

The use of such thermo-grams for the detection of breast cancer is often assisted by computational methods with dynamic or forced

changes in the body temperature, increasing the efficiency of the computational tools for mammothermography [2]. This kind of capture uses a combination of several thermo-grams acquired in a time interval and pattern recognition techniques. These techniques are especially efficient when dynamic protocol are used in acquiring the patient data [4]

In the dynamic protocol, before the beginning of the examination, the patients are cooled by an air streams, changing the temperature of their breast. They must be standup with the hands on the top of the head for 5 minutes; Figure 1 (a) shows this. Meanwhile, a series of images during they return to the thermal equilibrium with the environment are acquiring (Figure 1b shows some of this images).

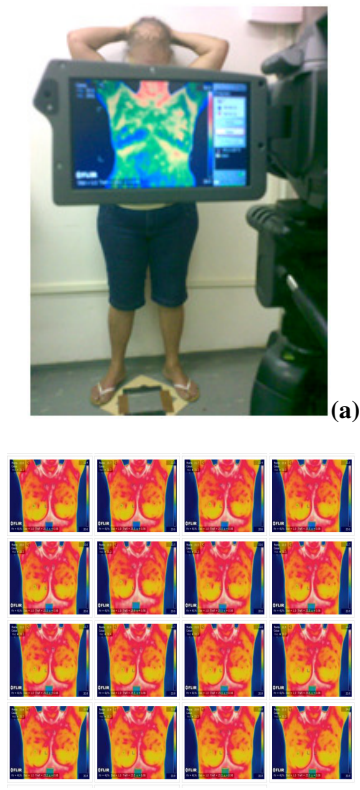


Figure 1: (a) Example of patient position during the thermo-gram examination and (b) samples of acquired images: thermo-grams.

However, during this 5 minutes, the patients breathe (inhale and exhale) doing some small movements. These change the coordinates of a point of their body in relation to the frame coordinates or to a fixed coordinates. Figure 2a shows the discrete points coordinate acquired in blue and the main patient coordinate system (real values) in red.

Such discrete points correspond to the Cartesian product of:  $(0, 1, \dots, N_1) \times (0, 1, \dots, N_2)$ . Figure 2b shows the movement of the nipples: the blue diamonds and read squares represent the right and left areola positions respectively, in a sequence of 20 frames in one of these examinations, when the area of the both breast as covered by a discrete grid of coordinates from  $(0,0)$  to  $(640,480)$ . When these differences of coordinates are not correct, they can results in error in the computational analyses. Therefore, approaches to correct or relate these points must be the first step in computational analyze of these thermo-grams.

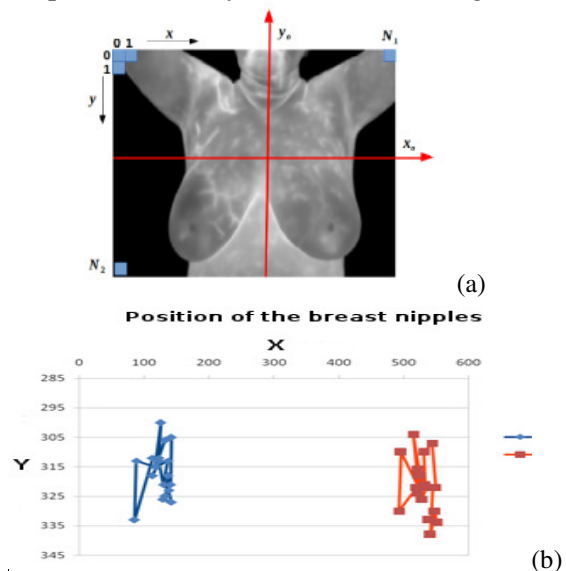


Figure 2: (a) Patient image in relation to the main body coordinate system, and (b) sample of the position of the nipples during the 5 minutes of examination.

Alignment among images that are taken at different times, coordinate systems or angles is named image registration [3]. It can be based on global or local registration methods and is fundamental in this kind of examinations [5].

Image registration matches all points in the scenes using various types of transformations from rigid bodies (translation and rotation), to non-rigid and even to nonlinear one [6]. However, the use of very generic or incorrect mathematical function to undo this displacements increase the processing time and even do not promote adequate results. To achieve a correct registration tool, useful for interactive and diagnostic system the first step must be to know the type of displacement that can correct the frame coordinate modification.

In this work, we studied the movements performed by the patient during dynamic acquisition and found a pattern of changes in the images sequence. We use a sequence of frames available in a public database in order to analyze the possible geometry of such movements [4]. From this observation, we find the possible locus of points of their body grouping them. In this way, two studies are performed: one identifying the movements performed by the patients and the other identifying the best model for transformation to be used in the mapping and the changes caused by such movements.

As results three types of displacements are defined as pattern: a lateral movement in the coronal plane; a forward-backward displacement; and a torsion deformation along her cranium-caudal axis. These movements were used to set hypothesis of changes in the sequence of images that was compared to a sequence of images of a mannequin to confirm the adopted hypothesis.

From this, it was found that the rotation and translation among a series of images of the same examination is the best function to be used in this registration mapping. The developed method to promote this statement

was tested in a heterogeneous group of 23 patients. In these, this mapping improve properly the alignment of all patients.

The rest of this article is organized as follow. Section 2 shows the study done on the sequence of frames of a public database. Section 3, comment about the hypothesis on the movements of the patients. Section 4 shows the comparison among patients (real) and the mannequin (rigid body) movements. The section 5 presents the test considering corrections by using rigid body mapping.

## 2. PATIENTS MOVEMENTS ANALYSIS

The analysis of the patients' movements is performed by observing several mammothermography stored in the DMR (Database for Mastologic Research) [7]. Considering the patients planes and axes of Figure 3 (that is the sagittal, coronal and transverse planes and the sagittal, longitudinal and transverse axes [8]), the differences among image of the same patient can be classified on three types of displacements: (1) a lateral movement in the coronal plane; (2) a forward-backward motion; and (3) a twist along the cranium-caudal axis.

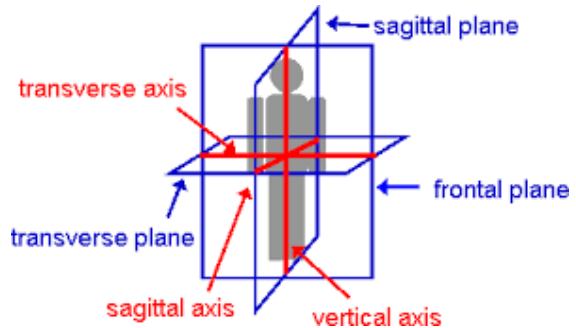
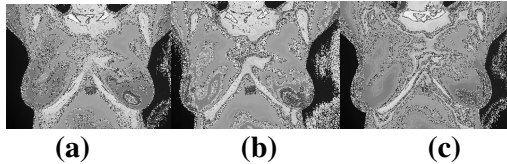


Figure 3: Anatomical planes and axes.

The first movement, lateral displacements, is mainly 2D. The patients continue on the coronal plane, by changing the angle (waist line) formed between the longitudinal and transverse

axes. This rotation can be in clockwise or counter-clockwise direction on the sagittal axis. Figure 4 shows an example of this movement: wherein Figure 4(b), the patient is slightly to the right relative to Figure 4(a) (initial position) and in Figure 4(c) both images are overlapped.



**Figure 4:** (a) First position, (b) patients with a slight angle to the right and (c) the two images overlapped.

The forward and backward displacements are performed in the sagittal plane, around an axis passing through the foot, parallel to the transversal axis. This movement occurs in front and rear direction of the patient, generating images such as those of Figure 5. Figure 5(a) is the first position. Figure 5(b) shows the patient with a slight tilt forward, reducing the distance to the camera and giving an idea that upper part of the patient's body has increased and the small square marker has moved up. This movement is emphasized in Figure 5(c), which superpose the edges of the Figure 5(a) and Figure 5(b).

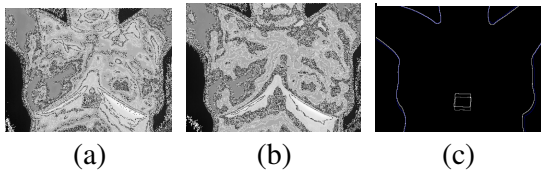


**Figure 5:** (a) A patient in the first position, (b) the patient lightly forwards (c) the edge of (a) and (b) superimpose.

The twisting around the longitudinal axis of the patients is represented in Figure 6. In the first image, Figure 6(a), the patient has a slight twist in a clockwise direction around the longitudinal axis. In Figure 6(b), it further

accentuates this movement. This movement is the cause of the lateral regions in red, below the left armpit of the patient, which appears in Figure 6(a) and is not present in Figure 6(b).

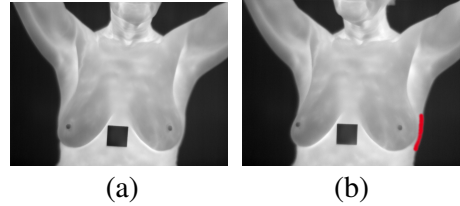


**Figure 6:** (a) Patient with light twist and (b) patient with more accentuated warping.

In addition to these three movements others not too common can be seen in the examinations, as the movement of the patient's head, which also can be seen in images of Figure 6. In Figure 6(a), the patient's chin is pointing forward and in Figure 6(b) her chin is pointing to right. However, this displacement of the head is not relevant for the breast examination, and is not considered for registration.

### 3. RIGID BODY MOTION X STRAIN

The motions, described in last section, can cause two types of changes in the acquired frames. At first, the whole body of the patient moves uniformly as a rigid body (rotations and translations), without deformations. In the second, the movement causes local changes in the patient's body and so deformations.

However, as the differences between the images are caused by movements which modify the body of the patient as a whole, it is possible to state that the major differences among images are caused by rigid transformations and local deformations are a secondary effect.

These assumptions can be verified by comparing the images acquired during the examination of a patient with images acquired by a mannequin, which is purposely positioned to simulate the same final position. But of course the mannequin always presents only rigid body displacements. Thus, if the acquired

images of the mannequin present similar or worse results than the patient, it confirms that the patient movements are mostly caused by rigid motion.

#### 4. PATIENT DEFORMATION X MANNEQUIN DISPLACEMENTS

In order to produce a fair comparison among the images of the patient and mannequin, its images are acquired by using the same thermal camera, with same size and resolution used for the patients. The only difference is that the images of the mannequin are acquired in the visible range while the patient's frames are in the infrared frequency.

The analysis is made through consideration of the coordinates of four points manually identified and present in all the images of the patient or mannequin. In the patient's images, the points analyzed are highlighted in red in Figure 7(a): the two nipples and lower point of the inframammary lines. In the mannequin, the same points were marked with blue before the image acquisition, as shown in Figure 7(b).

In the mannequin or patient images, two segments of lines are considered. One is defined by the nipples and the second by connecting lower points of the inframammary line. These two lines are almost parallel, and represented by the blue lines on the images of Figure 7. Through these segments, we can simulate in the mannequin pseudo deformations like those observed in the sequences of the examination. They are calculated by the size of the segments that changes along a sequence of acquisition.

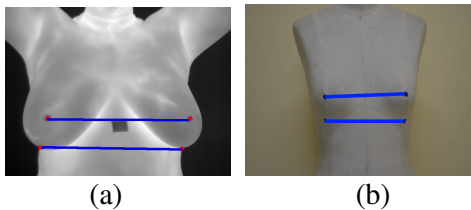


Figure 7: Points and lines used for definition of the displacements in the patient examination (a) and (b) pseudo deformation in the mannequin.

Equation (1) represents the deformation of the line segment in the position  $i$ , that has final length  $l_i$ , and initial length  $l_1$ . Where the lengths are calculated by the Euclidean distance between the end points of each line. For both, the patient and mannequin images, the pixels of the frame are organized inside a discrete and closed set  $\Omega$ , subset of  $Z^2$ , with integer elements  $\omega = (x, y)$ , where  $0 \leq x \leq 639$  and  $0 \leq y \leq 479$ .

$$\epsilon_i = (l_i - l_1) / l_1 \quad (1)$$

An example of the deformation achieved by a patient examination can be seen in Table 1. In it, each line represents an image of the patient and the columns,  $l_i$  and  $\epsilon_i$ , are the segment length in the image  $i$  and the segment deformation in relation to first image  $l_1$ . Deformations in the nipples and in the inframammary folds level are considered.

Table 1 suggests possible deformations on segments between the nipples, the greater deformation was -0.035 in the image 7, indicating that, in this image; the upper segment decreased 3.5% compared to the first image size. At the level of the inframammary folds, the largest deformation was -0.060 in image 4, indicating that, in this image, the lower segment decreased 6% compared to the first image size. Similar study is done in mannequin images. The results obtained with the upper and lower line segments of the mannequin are presented in Table 2. At the upper lines, the mannequin greater deformation is measured on image 8 and is 0.15, indicating a pseudo increase of 15% of the segment length in this image. At the inframammary level, the largest deformation was also 0.15 in the image 8. The greater deformations for the mannequin are 15% even greater than those of the patients.

**Table 1: Results of the deformation of the line segment in the patients' images**

Frame	Position	$l_i$	$\epsilon_i$
1	Nipples	403.0	0
	Infr. folds	403.0	0
2	Nipples	408.0	0.012
	Infr. folds	407.0	-0.010
3	Nipples	402.0	-0.003
	Infr. folds	402.0	-0.002
4	Nipples	399.1	-0.010
	Infr. folds	380.1	-0.060
5	Nipples	398.0	-0.012
	Infr. folds	388.0	-0.039
6	Nipples	402.0	-0.002
	Infr. folds	390.0	-0.033
7	Nipples	389.0	-0.035
	Infr. folds	391.0	-0.031
8	Nipples	406.1	0.008
	Infr. folds	389.0	-0.036
9	Nipples	408.0	0.012
	Infr. folds	392.1	-0.028
10	Nipples	408.0	0.012
	Infr. folds	387.2	-0.041
11	Nipples	407.1	0.010
	Infr. folds	405.0	0.005
12	Nipples	410.1	0.018
	Infr. folds	390.0	-0.033
13	Nipples	399.0	-0.010
	Infr. folds	385.0	-0.047
14	Nipples	402.0	-0.002
	Infr. folds	386.0	-0.044
15	Nipples	408.0	0.012
	Infr. folds	391.0	0.031
16	Nipples	408.0	0.012
	Infr. folds	395.0	-0.020
17	Nipples	408.2	0.013
	Infr. folds	397.0	-0.015
18	Nipples	410.1	0.013
	Infr. folds	388.0	-0.039
19	Nipples	409.1	0.015
	Infr. folds	391.0	-0.031
20	Nipples	408.1	0.013
	Infr. folds	392.0	-0.028

From the previous two tables, it is clear that, in a similar way both patient and mannequin images could be under the same deformation of upper and bottom line segments. Moreover, for the mannequin these deformations are more significant than for the patient. Finally, similar to the thermal image, the mannequin images can also be of compression and traction, meaning pseudo increases and decreases in the

sizes of the segments.

**Table 2: Results of the deformation of the line segments in the mannequin images.**

	Position	$l_i$	$\epsilon_i$
1	Nipples	224.1	0
	Infr. folds	223.5	0
2	Nipples	212.4	-0.05
	Infr. folds	211.4	-0.05
3	Nipples	208.0	-0.07
	Infr. folds	216.7	-0.03
4	Nipples	254.9	0.14
	Infr. folds	247.2	0.11
5	Nipples	252.2	0.13
	Infr. folds	243.8	0.09
6	Nipples	215.3	-0.04
	Infr. folds	211.0	-0.05
7	Nipples	216.0	-0.04
	Infr. folds	213.4	-0.04
8	Nipples	258.0	0.15
	Infr. folds	256.3	0.15

As the mannequin is made of a rigid material, which performed only rigid displacements, and the deformations obtained using the equation (1) were higher than those from the images to the patient, the hypothesis of the representation of the patient's motion as a rigid body is a valid assumption. To reinforce it, a visual comparison is made among the quadrilaterals formed by the points of the images. Through these the changes in each image were checked and compared visually.

#### 4.1 Comparison of the quadrilateral of patient and mannequin

The four points analyzed in all images of the patient are represented in Figure 8, where their abscissas and ordinates are related to the coordinates  $x$  and  $y$  of  $\Omega$ .

The quadrilaterals formed by the points analyzed from the images of the mannequin are displayed on the graph of Figure 9. The mannequin points have greater difference than those of the patient.

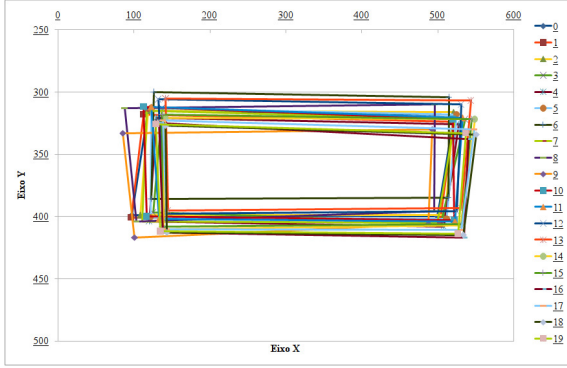


Figure 8: Quadrilateral formed by the points in the patients images

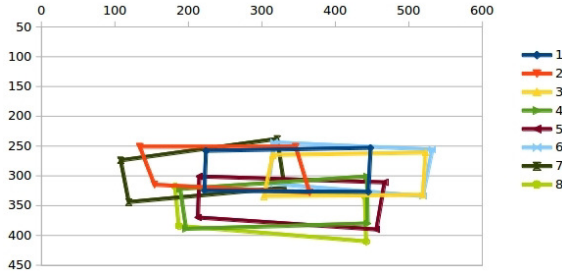


Figure 9: Quadrilateral formed by the points in the mannequin images

## 5. MODEL FOR IMAGES ALIGNMENT

As the differences between body points and their coordinates in the frames can cause errors in the analysis of temperatures, before being analyzed these points must be aligned. Frame matching is done by image registration, that is the process of finding a function between similar points in two images: sensitive and reference, creating a mapping (or transformation), which changes the points in the sensitive image making it more similar to the reference one. However, to achieve a correct alignment it is necessary to choose the correct transform. Several previous studies have used different types of transform from linear function to the nonlinear ones [6] as:

$$\Phi: \Omega \rightarrow \Omega \quad (2)$$

where  $\Omega$  are the set of image points.

### 5.1 Choosing the transformation.

In section 4, it is observed that the displacements of the patients on their thermal examinations can be treated as a rigid body movement, because altering the alignment between the patient and the camera there are images with similar aspect of (pseudo) deformation.

Images of different views of the same scene can be mapping through the transformation of projections or affine transformations [9]. When the camera is far from the body is better to use of affine transformations, and when they are close, the use of projective transformation is the best option.

Affine transformations preserve the straight lines of the set and the existing parallelism between them [10]. However, angles between lines and the distances between points are not necessarily constant under such transformations. Affine transformations can do translation, scale, rotation, reflection and shear.

If  $\omega=(x,y)$ , and  $\omega \in \Omega$  then an affine transformation is expressed as in Equation (3), where  $a_1$ ,  $a_2$ ,  $a_3$  and  $a_4$  are real numbers (linear part),  $t_x$  and  $t_y$  are real numbers that do the translation

$$\Phi\left(\begin{matrix} x \\ y \end{matrix}\right) = \begin{bmatrix} a_1 & a_2 \\ a_3 & a_4 \end{bmatrix} * \begin{bmatrix} x \\ y \end{bmatrix} + \begin{bmatrix} t_x \\ t_y \end{bmatrix} \quad (3)$$

Other type of transformation is the rotations [9]. This class of transformations presents  $a_1=a_4= \cos \alpha$  and  $a_2=-a_3= \sin \alpha$ . In this type of transformation the straight lines and the parallelism between them are preserved. During tests carried out by a previously register created in Galvão *et al* [11], it was noticed that in some cases, less generic transformations can produce better results than those with a higher degree. This is primarily because the relatively large number of parameters to be calculated in the more general transformations can generate greater errors when the images can be aligned

by the lower mobility functions. Therefore, it is expected that both the translations plus rotations align properly the images of patients.

## 5.2 Test of the transformation functions.

To find out if the two transformations works for our application, tests are carried out on patients' images using both transformations. The level of misalignments of the images is calculated before and after the image registration by each type of transformation (affine and rigid body). The results are compared and analyzed. For more reliable comparison, the registration methods used in this verification are guided by the same characteristics and its transformation functions are calculated by the same techniques. The only difference between the two registrations is the adopted transformation. As each examination presents 20 thermograms, all images match the first image of the sequence. Thus, in each test, 19 comparisons are performed, the first image with second image, the first with third and so on.

## 6. CONCLUSIONS

This study aims to assist the methods of image registration for infrared exam. It considers transformation functions that can align images and improve computing analyze. The movement of the patient was analyzed and compared with movements of mannequin. This points the transformation functions to be chosen and tested. The movements of the patients were analyzed from public available images [4]. In these, we noted that the major movements of the patients can be divided in three set: (1) a lateral movement in the coronal plane; (2) a forward-backward motion; and (3) a twist along the cranium-caudal axis. Then, we deduced that the patients' movements can be described as a rigid body transformation. To confirm that the patient's movements can be considered as translation and rotations, a mannequin images performing equivalents

displacements are considered. Points were observed both in the patients and mannequin images and the level of deformation was calculated. From this study we noted that the mannequins' images have more displacements than the patients' images. Confirming the patients' images deformation can see as rigid body movements of the patients. In resume, we can say that these transformations are enables to improve the aligning of the patients' images and that the displacements of images are caused mainly from the rigid body movements.

## ACKNOWLEDGMENTS

The authors acknowledge CNPq and CAPES for funding this work.

## REFERENCES

- [1] J. P. Agnelli, A. B. Cristina and V. Turner, "Tumor Location and Parameters Estimation by Thermography", *Mathematical and Computer Modeling*, 53(7-8):1527-1534, 2011.
- [2] Liu and Z. S. Deng, "Numerical Methods for Solving Bioheat Transfer Equations in Complex Situations", *Advances in Numerical Heat Transfer*, 3(3):75-120, 2009.
- [3] M. Petrou, "Image Registration: an overview", *Advances in Imaging and Electron Physics*, 130:243-291, 2004.
- [4] L. F. Silva, D. C. M. Saade, G. O. Sequeiros, A. C. Silva, A. C. Paiva, R. S. Bravo and A. Conci, "A new database for mastology research with infrared image", *Journal of Medical Imaging and Health Informatics - Volume 4, Number 1 (March 2014)* pp.92 - 100.
- [5] K. B. Siti and M. Petrou, "Elastic image registration for landslides monitoring. *International Journal of Signal Processing*,

- Image Processing and Pattern Recognition, 3(3), 2010.
- [6] Zitova, J. Flusser and F. Sroubek, Image Registration: a survey and recent advances, ICIP Tutorial, Genoa, Italy, 2005.
- [7] Silva, L. F., Saade, D. C. M., Sequeiros, G. O., Silva, A. C., Paiva, A. C., Bravo, R. S., Conci, A., A New Database for Breast Research with Infrared Image. Journal of Medical Imaging and Health Informatics, 4(1): 92-100, 2014.
- [8] [https://en.wikipedia.org/wiki/Anatomical\\_plane](https://en.wikipedia.org/wiki/Anatomical_plane)
- [9] Goshtasby, A. A, 2-D and 3-D Image registration. John Wiley & Sons. Ed. 1. 2005
- [10]Ho, J. and Yang, M., On affine registration of planar point sets using complex numbers. Computer Vision and Image Understanding (1)115: 50-58.
- [11]Galvão, S., Marques, R., Conci, A., Sanchez, A., A registration method for IR images: Preserving the thermal breast characteristics In *Proceedings of International Conference on Systems, Signals and Image Processing*, 2013, Bucarest. v. 1. p. 147-150.